Free Vibration of Fiber Composite Thin Shells in a Hot Environment

PASCAL K. GOTSIS* AND JAMES D. GUPTILL
National Aeronautics and Space Administration
Lewis Research Center
Cleveland, OH 44135

ABSTRACT: Results are presented of parametric studies to assess the effects of various parameters on the free vibration behavior (natural frequencies) of $[\pm\theta]_2$ angle-ply fiber composite thin shells in a hot environment. These results were obtained by using a three-dimensional finite element structural analysis computer code. The fiber composite shell is assumed to be cylindrical and made from T300 graphite fibers embedded in an intermediate-modulus high-strength matrix (IMHS). The residual stresses induced into the laminated structure during the curing are taken into account. The following parameters are investigated: the length and the thickness of the shell, the fiber orientations, the fiber volume fraction, the temperature profile through the thickness of the laminate and the different ply thicknesses. Results obtained indicate that: the fiber orientations and the length of the laminated shell had significant effect on the natural frequencies. The fiber volume fraction, the laminate thickness and the temperature profile through the shell thickness had a weak effect on the natural frequencies. Finally, the laminates with different ply thicknesses had insignificant influence on the behavior of the vibrated laminated shell.

KEY WORDS: laminated cylinders, fiber composites, angle-ply laminates, composite structures, computational simulation, residual stresses, high temperature, moisture, structural analysis, finite element analysis, free vibration, natural frequencies, mode shape.

INTRODUCTION

HIGH SPEED FLIGHT vehicles under hostile environments at speeds which are multiples of the speed of sound require new materials and improved computational approaches to design them. New materials, known as elevated temperature composites, have high strength, are light in weight, and can be tailored for specific performance requirements. These materials are already finding applications and acceptance in aircraft frame and engine structures. Cost effective usage of elevated temperature composite materials requires new ideas and innovative concepts in the areas of material selection and structure fabrication in order to design for durability by properly accounting for many failure mechanisms in-

*Author to whom correspondence should be addressed.

Reprinted from *Journal of* REINFORCED PLASTICS AND COMPOSITES, *Vol. 14—February 1995*

herent in composites. The influence of hostile environments, nonlinear material and structural behavior, and the coupling between responses induced by various loads require sophisticated analysis methods.

A stand-alone multi-disciplinary computer code, CSTEM (Coupled Structural/Thermal/Electro-Magnetic Analysis/Tailoring) [1 to 5] has been developed by integrating three-dimensional finite element structural/stress analysis methods with several single-discipline codes including those for integrated composite mechanics [6,7].

This paper demonstrates the use of CSTEM to computationally simulate aircraft engine composite structures subjected to free vibration at elevated temperatures. Knowledge of the natural frequencies of structures is important in considering their response to various kinds of excitation especially when structures and force systems are complex and when excitations are not periodic [8,9]. The structure studied is a thin, cylindrical composite shell. The composite is to be made from angle-ply $[\pm\theta]_2$ laminates containing plies with uniform thickness. The residual stresses induced into the laminated composite during the curing process are taken into account. Parametric studies were performed to examine the effects on the natural frequencies of parameters such as: the length and the laminate thickness of the shell, the temperature profile through the thickness of the laminate, the fiber volume fraction, the fiber orientations and laminates with different ply thicknesses.

BRIEF DESCRIPTION OF THE SIMULATION PROCEDURE

The general purpose computer program CSTEM [1] computationally simulates the coupled multidisciplinary structural, heat transfer, vibration, acoustic, and electromagnetic behavior of elevated temperature, layered multi-material composite structures in aggressive environments. All the disciplines are coupled for nonlinear geometrical, material, loading, and environmental effects. CSTEM is based on a modular structure, (Figure 1), and is accessed by the user through its executive module. The structural response can be predicted at all the composite scales including constituents (fiber and matrix) and ply level.

The composite mechanics is simulated with the ICAN (Integrated Composite Analysis) module [6,7], which performs, among others, through-the-thickness point stress analysis. The micro-mechanics equations embedded in ICAN include the effects of temperature and moisture. ICAN simulates the behavior of polymer composites from the constituent material level to the laminate level as depicted in Figures 2 and 3. ICAN includes a resident material property data bank for commercially available fiber and matrix constituent materials at room temperature. The user needs only to specify a code name for the desired constituent materials (rather then having to manually input all the properties) in the CSTEM input.

The procedure to computationally simulate composite structures is shown in Figure 2 and consists of four parts: the constituents, the synthesis, the finite element structural analysis, and the decomposition. For detailed description of these four parts see References [6] and [7]. The computational procedure steps are:

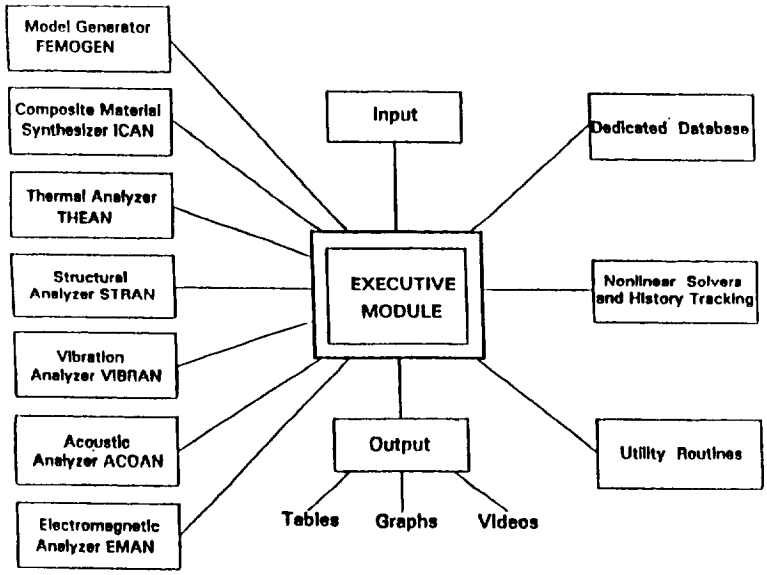

Figure 1. *CSTEM modular structure.*

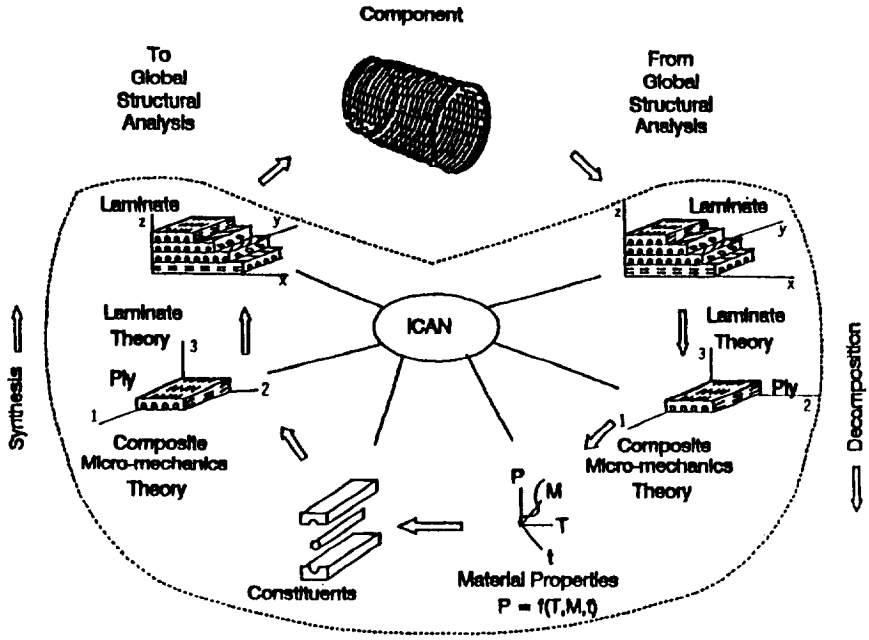

Figure 2. *Integrated composite analysis.*

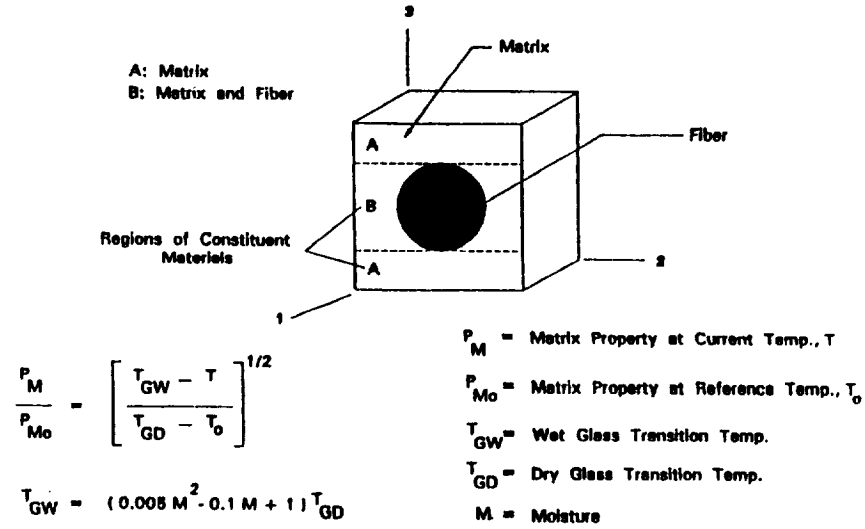

Figure 3. Regions of constituent materials and nonlinear material characterization model.

1. *Constituents*—The material properties of the matrix, in any operational temperature and moisture condition are updated based on the constitutive equation depicted in Figure 3.
2. *Synthesis*—The thermal and mechanical properties of the plies are synthesized knowing the mechanical properties of the fibers and the matrix using composite micro-mechanics theory.

   The extensional stiffness matrix A, the coupling stiffness matrix B, and the bending stiffness matrix D are computed by using the laminate theory as well as the effective laminate thermal and mechanical engineering properties [10].
3. *Finite Element Analysis*—The finite element analysis is performed at the composite structure scale, and among the others, the resulting forces and moments are computed at each node of the finite element mesh. Because ICAN performs through-the-thickness point stress analysis, steps (1) and (2), as well as (4) are performed at each individual node of the finite element mesh.
4. *Decomposition*—The stresses and strains in each ply are computed by using the laminate theory. The stresses and strains in the matrix and the fibers for each ply are computed by using composite micromechanics.

The CSTEM code is written in the FORTRAN programming language and installed on the NASA Lewis CRAY-YMP computer system.

SUMMARY OF THE BASIC EQUATIONS

Ply Level Equations

It is assumed that the heterogeneous ply consisting of fibrous and matrix

phases can be modeled as a homogeneous and orthotropic medium. Also, the ply is assumed to be subjected to a state of plane stress. The stress strain relationship for the kth ply in material axes 1, 2, 3 (1 is the direction of the fibers and 3 is the direction normal to the 1, 2 plane) is the following:

$$\{\sigma_L\} = [Q_L](\{\epsilon_L\} - \{\epsilon_L\}_T - \{\epsilon_L\}_M) \tag{1}$$

where

$$\{\sigma_L\}^T = [\sigma_1, \sigma_2, \sigma_{12}],$$

$$[Q_L] = \begin{bmatrix} Q_{11} & Q_{12} & 0 \\ Q_{21} & Q_{22} & 0 \\ 0 & 0 & Q_{33} \end{bmatrix}$$

and $Q_{11} = E_1/P$, $Q_{22} = E_2/P$, $Q_{12} = Q_{21} = \nu_{12} E_1/P = \nu_{21} E_2/P$, $Q_{33} = G_{12}$ and $P = 1 - \nu_{12}\nu_{21}$. The effective properties of the kth ply, E_1, E_2, ν_{12}, ν_{21} and G_{12} are computed analytically from the constituent material properties (the fiber and the matrix) [6,7].

$\{\epsilon_L\}^T$ = $[\epsilon_1\ \epsilon_2\ \gamma_{12}]$ is the mechanical strain vector
$\{\epsilon_L\}_T^T$ = $[a_1\ a_2\ 0]\Delta T$ is the thermal strain vector and
$\{\epsilon_L\}_M^T$ = $[\beta_1\ \beta_2\ 0]\Delta M$ is the moisture strain vector
a_1 and a_2 = the effective free thermal expansion coefficients of the kth ply with respect to the 1- and 2-axes
β_1 and β_2 = the effect free moisture expansion coefficients of the kth ply with respect to 1- and 2-axes
ΔT = the temperature in the kth ply
ΔM = the moisture in the kth ply.

From Equation (1) we have:

$$\{\sigma_L\} = [Q_L](\{\epsilon_L\}) = \{\sigma_L\}_T - \{\sigma_L\}_M \tag{2}$$

where

$[Q_L]\{\epsilon_L\}$ = the mechanical stress vector
$\{\sigma_L\}_T$ = the thermal stress vector
$\{\sigma_L\}_M$ = the moisture stress vector

Next, Equation (2) is transformed from the material axes 1, 2, 3 to the laminated axes x, y and z (the z-axis coincides with the 3-axis) using the rotational transformations as following:

$$\{\sigma\} = [T]^{-1}\{\sigma_L\}_T$$

$$[Q] = [T]^{-1}[Q_L][T]$$

$$\{\epsilon\} = [T]^{-1}\{\epsilon_L\}$$

$$\{\sigma\}_j = [T]^{-1}\{\sigma_L\}_j$$

for $j = T, M$.

$$[T] = \begin{bmatrix} m^2 & n^2 & 2mn \\ n^2 & m^2 & -2mn \\ -mn & mn & m^2 - n^2 \end{bmatrix}$$

$$[T]^{-1} = \begin{bmatrix} m^2 & n^2 & -2mn \\ n^2 & m^2 & 2mn \\ mn & -mn & m^2 - n^2 \end{bmatrix}$$

where $m = \cos\theta$, $n = \sin\theta$ and θ = the angle between the 1- and x-axes. Thus, Equation (2) can be written in the form:

$$\{\sigma\} = [Q]\{\epsilon\} - \{\sigma\}_T - \{\sigma\}_M \tag{3}$$

Laminate Level Equations

The strain-displacement relationship of the laminate at a distance z from the midplane of the laminate is:

$$\{\epsilon\} = \{\epsilon^0\} + z\{k\} \tag{4}$$

where

$\{\epsilon\}^T = [\epsilon_x \epsilon_y \gamma_{xy}]$
$\{\epsilon^0\} = [\epsilon_x^0 \epsilon_y^0 \gamma_{xy}^0]$ is the strain vector at the midsurface of the laminate
$\{k\}^T = [k_x k_y k_{xy}]$ is the curvature vector at the midsurface of the laminate

Substituting Equation (4) into Equation (3) we obtain the following:

$$\{\sigma\} = [Q]\{\epsilon^0\} + z[Q]\{k\} - \{\sigma\}_T - \{\sigma\}_M \tag{5}$$

The vectors of the resultant forces and moments act at the midplane of the laminate with thickness h, and can be written in the following form:

$$\{N\} = \int_{-h/2}^{h/2} \{\sigma\} dZ \tag{6}$$

$$\{M\} = \int_{-h/2}^{h/2} \{\sigma\} z dz \tag{7}$$

By substituting the ply stresses of the kth ply of Equation (5) into Equations (6) and (7) we finally obtain:

$$\left\{\begin{matrix} N \\ M \end{matrix}\right\} = \left[\begin{array}{c|c} A & B \\ \hline B & D \end{array}\right] \left\{\begin{matrix} \epsilon^0 \\ k \end{matrix}\right\} - \left\{\begin{matrix} N \\ M \end{matrix}\right\}_T - \left\{\begin{matrix} N \\ M \end{matrix}\right\}_M \tag{8}$$

where $[A]$ is the extensional stiffness matrix, $[B]$ is the coupling stiffness matrix and $[D]$ is the bending stiffness matrix and are defined as following

$$[A] = \int_{-h/2}^{h/2} [Q]_k dz = \sum_{K=1}^{n} \int_{h_{K-1}}^{h_K} [Q]_K dz = \sum_{K=1}^{n} [Q]_k (h_K - h_{K-1})$$

$$[B] = \int_{-h/2}^{h/2} [Q]_k z dz = \sum_{K=1}^{n} \int_{h_{K-1}}^{h_K} [Q]_K z dz = \frac{1}{2} \sum_{K=1}^{n} [Q]_K (h_K^2 - h_{K-1}^2)$$

$$[D] = \int_{-h/2}^{h/2} [Q]_k z^2 dz = \sum_{K=1}^{n} \int_{h_{K-1}}^{h_K} [Q]_K z^2 dz = \frac{1}{3} \sum_{K=1}^{n} [Q]_K (h_K^3 - h_{K-1}^3)$$

where n is the number of the plies in the laminate.

In order to perform the structural analysis of the fiber composite structure, it is required to know the mechanical and thermal properties of the laminate. Therefore the laminate is treated as homogeneous and possessing effective laminate engineering properties which are described in details in Reference [10].

Structural Level Equations

The equations of equilibrium governing the linear dynamic response of the structure written in a matrix form are the following [8,9]:

$$[M]\{\ddot{U}\} + [D]\{\dot{U}\} + [K]\{U\} = \{R(t)\} \tag{9}$$

where

$[M]$ = the structural mass matrix
$[D]$ = the structural damping matrix
$[K]$ = the structural stiffness matrix
$\{R(t)\}$ = the external applied load vector, as a function of time
$\{U\}$ = the displacement vector
$\{\dot{U}\}$ = the velocity vector
$\{\ddot{U}\}$ = the acceleration vector

The equilibrium Equations (9), in the case of the free vibration problem are

simplified by setting the force vector equal to zero, $\{R(t)\} = 0$. If the damping effect is not taking into account then the damping matrix is equal to zero, $[D] = 0$. The equilibrium equations are simplified as following:

$$[M]\{\ddot{U}\} + [K]\{U\} = 0 \tag{10}$$

The structural matrices $[M]$ and $[K]$ are computed as follows: the continuous structure is discretized in a number of finite elements. If $[H]$ is the shape function of a finite element of the structure then:

(a) the mass matrix of an element is given by the equation:

$$[m] = \int_V \varrho [H]^T [H] dV$$

where ϱ is the mass density of the element of the structure.

(b) The stiffness matrix of an element is given by the equation:

$$[k] = \int_V [B]^T [C][B] dV$$

where $[C]$ is the material matrix of the element, which contains the anisotropic effective properties of the laminate and is related to the stress-strain relationship as following:

$$\{\sigma\} = [C]\{\epsilon\}$$

The matrix $[B]$ is related to the strain displacement relationship as following:

$$\{\epsilon\} = [B]\{u\}$$

where $[B] = [L][N]$, $[L]$ is a linear operator and $[N]$ is the matrix which consists of the shape functions $[H]$ [12].

The structural mass matrix $[M]$ is assembled from the element mass matrices $[m]_j$ for $j = 1, nel$, where nel is the number of finite elements in the structure. Similarly, the structural stiffness matrix $[K]$ is assembled from the element stiffness matrices $[k]_j$, $j = 1, nel$.

After the computation of the $[M]$ and $[K]$ matrices the next step is to solve Equation (10). The solution of Equation (10) can be postulated to be of the following form:

$$\{U\} = \{\varphi\} \sin \omega(t - t_0) \tag{11}$$

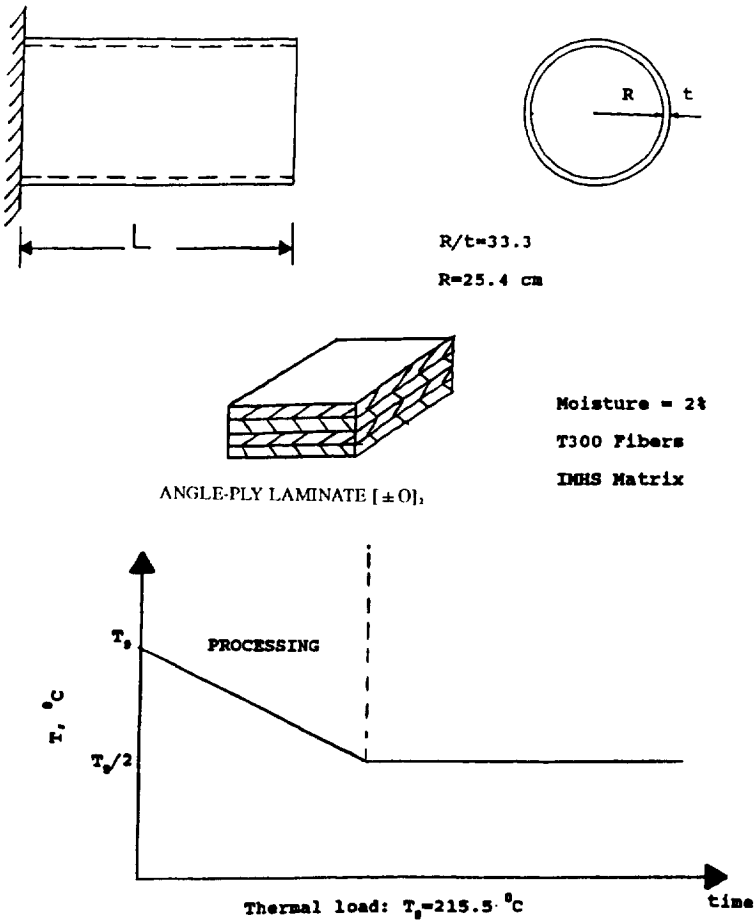

Figure 4. *Geometry, materials and processing of laminated cylinder.*

Substituting Equation (11) into Equation (10) we obtain the following:

$$[K]\{\varphi\} = \omega^2[M]\{\varphi\} \tag{12}$$

For the computation of the vibration frequencies (eigenvalues) and the mode shapes (eigenvectors), CSTEM incorporates the following two methods: the determinant search and subspace iteration [9,11]. The search method is intended more for a small number of equations, while subspace iteration is more efficient for a large number of equations.

GEOMETRY, LOAD HISTORY AND FINITE ELEMENT MODEL OF THE LAMINATED SHELLS

The fiber composite thin shell had a cylindrical geometry with the following dimensions. The ratio of the longitudinal length L to the inner radius R was equal to $L/R = 4$. The ratio of the inner radius R to the thickness t of the shell was $R/t = 33.3$. The radius R was 25.4 cm. The boundary conditions were fixed at one end and free at the other (Figure 4). The laminate consists of continuous fibers made of the graphite material T300 embedded in intermediate modulus high-strength (IMHS) matrix. The material properties of the fiber and the matrix were taken from the data bank available in CSTEM (Tables 1 and 2, respectively). The fiber volume fraction (FVR) was 55 percent and the moisture content was 2 percent. A balanced and symmetric laminate was assumed with fiber orientations of $[\pm\theta]_2$ and plies of equal thickness.

The simulation of the processing of the laminated cylinder was taken into account. It started from the curing temperature T_g of the matrix equal to 215.5°C (Table 2) and gradually reduced until the oeprating temperature was equal to $T_g/2$ (Figure 4). At the end of the processing, residual stresses were induced in the constituent materials of the composite structure.

For the free vibration analysis of the shell structure the effect of damping was neglected. The computational simulation was performed using three dimensional

Table 1. T300 graphite fiber properties at room temperature

Modulus in longitudinal direction, GPa	220.7
Modulus in transverse direction, GPa	13.79
In-plane Poisson's ratio	0.20
Out-of-plane Poisson's ratio	0.25
In-plane shear modulus, GPa	8.96
Out-of-plane shear modulus, GPa	4.827
Thermal expansion coefficients in longitudinal direction, 10^{-6} mm/(mm-°C)	0.99
Thermal expansion coefficients in transverse direction, 10^{-6} mm/(mm-°C)	10.00
Thermal conductivity in longitudinal direction, W/(m-K)	83.69
Thermal conductivity in transverse direction, W/(m-K)	8.369
Fiber tensile strength, GPa	2.413
Fiber compressive strength, GPa	2.069

Table 2. IMHS matrix properties at room temperature

Modulus in longitudinal direction, GPa	3.448
Modulus in transverse direction, GPa	3.448
In-plane Poisson's ratio	0.35
Out-of-plane Poisson's ratio	0.35
Thermal expansion coefficients in longitudinal direction, 10^{-6} mm/(mm-°C)	64.8
Thermal expansion coefficients in transverse direction, 10^{-6} mm/(mm-°C)	64.8
Thermal conductivity in longitudinal direction, *W*/(m-K)	2.16
Thermal conductivity in transverse direction, *W*/(m-K)	2.16
Matrix tensile strength, MPa	103.4
Matrix compressive strength, MPa	241.3
Matrix shear strength, MPa	89.6
Void fraction	0.225
Glass transition temperature, °C	215.55

finite element analysis. One (eight node) element through the thickness of the composite shell structure was used. The finite element mesh consists of 760 nodes and 360 elements (Figure 5).

RESULTS AND DISCUSSION

In this section results obtained for the different $[\pm\theta]_2$ angle-ply composite shells are presented and discussed. The parameters investigated include:

1. effects of fiber orientations
2. effects of cylinder length
3. effects of laminate thickness
4. effects of temperature
5. effects of fiber volume fraction
6. effects of different ply thicknesses

Effects of Cylinder Length

The influence of the cylinder length in conjunction with the ply angle θ was examined to study the free vibration behavior of the composite shell. Results obtained for natural frequencies and mode shapes are summarized below.

THE NATURAL FREQUENCIES

Three thin composite shells with different length ratios *L/R* of 2, 4, and 6 were examined. The computed values of the first natural frequency is plotted versus the ply angle θ and the three *L/R* ratios in Figure 6. The computed values are normalized with respect to the maximum frequency of 554.9 cps. Correspondingly, the values of the second frequency are normalized with respect to the maximum frequency of 609.6 cps and are plotted in Figure 7. Finally, the values of the third frequency are normalized with respect to the maximum frequency of 871.8 cps and are shown in Figure 8. The following conclusions are reached.

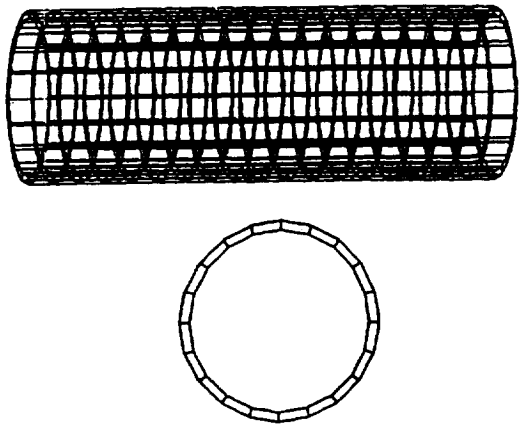

Figure 5. *Three dimensional finite element mesh and transverse cross sectional area of laminated shell structures.*

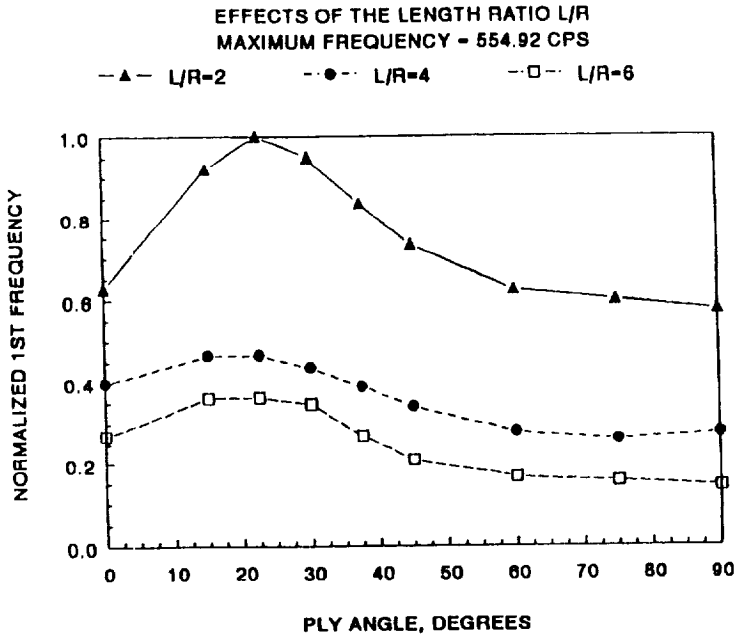

Figure 6. *Influence of the cylinder length on the lowest frequency of the laminated shell. R/t = 33.3, FVR = 55%, moisture = 2%.*

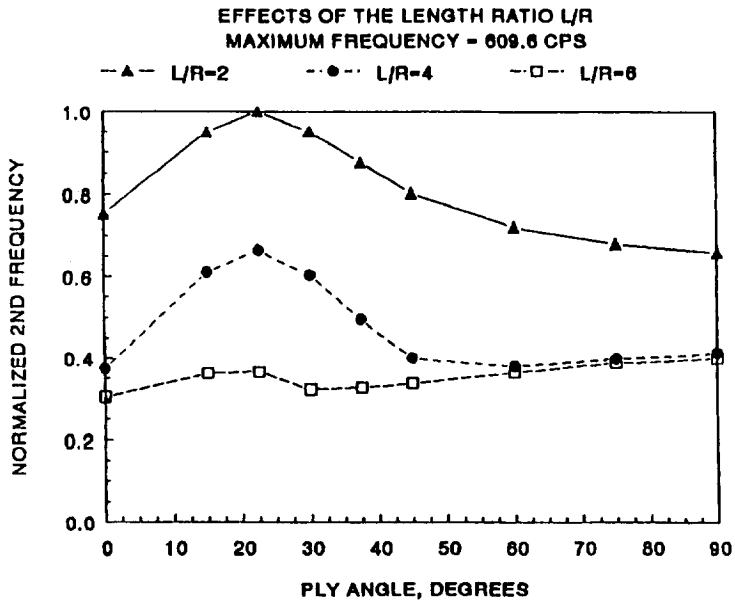

Figure 7. *Influence of the cylinder length on the second frequency of the laminated shell.*

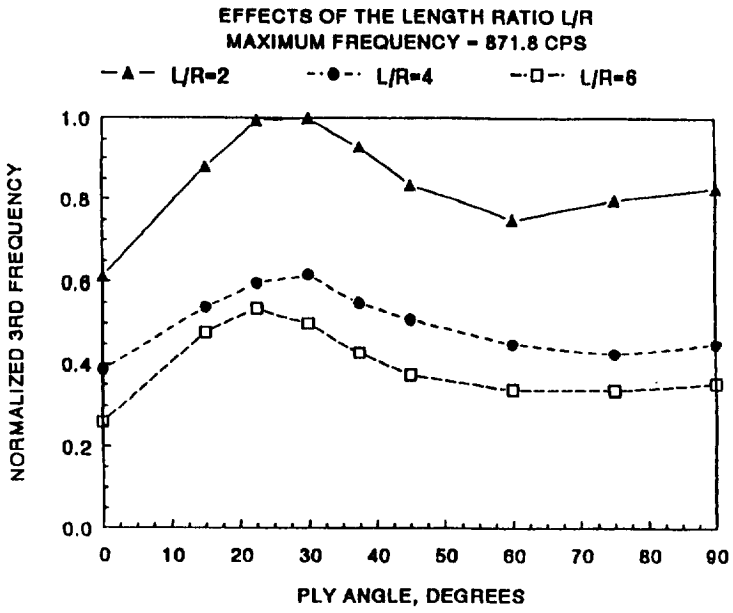

Figure 8. *Influence of the cylinder length on the third frequency of the laminated shell.*

Table 3. The percent difference in the natural frequencies between the short (L/R = 2) and the long (L/R = 6) cylinders.

Freq.	$[0]_4$	$[\pm 15]_2$	$[\pm 30]_2$	$[\pm 45]_2$	$[\pm 60]_2$	$[\pm 75]_2$	$[\pm 90]_2$
First	57%	60.7%	63.5%	70.7%	73.3%	74.1%	75.4%
Second	60%	59.6%	67%	65.9%	63.5%	55.7%	40%
Third	58%	45.4%	50%	55.4%	54.9%	57.7%	57.3%

$$\text{Percent difference} = \frac{\text{Frequency } (L/R = 2) - \text{Frequency } (L/R = 6)}{\text{Frequency } (L/R = 2)} \cdot 100\%$$

1. For all L/R, the natural frequencies increased for $0 \leq \theta \leq 22.5$ and decreased for $22.5 \leq \theta \leq 90$. The maximum frequencies (first, second and third) occurred at $\theta = 22.5$.
2. The shorter the shell the higher the frequencies as expected, since shorter shells are stiffer than the longer shells.
3. The percent difference of the natural frequencies between the short ($L/R = 2$) and the long ($L/R = 6$) shells for the different ply angles are tabulated in Table 3. It is seen that the percent difference of these natural frequencies is significant and dependent on the ply orientation angle.

THE MODE SHAPES

The behavior of the mode shapes of the composite shell with $L/R = 6$ and $R/t = 33.3$ for the first three frequencies are presented graphically as follows:

1. First frequency (lowest frequency): the mode shape of the first frequency is shown in Figure 9. It is primarily bending indicating that the shell behaves like a cantilever beam.

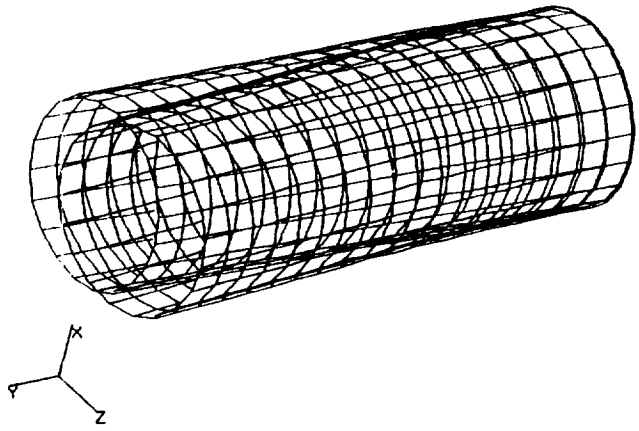

Figure 9. *The first mode shape of the $[\pm\theta]_2$ angle-ply laminated shell.*

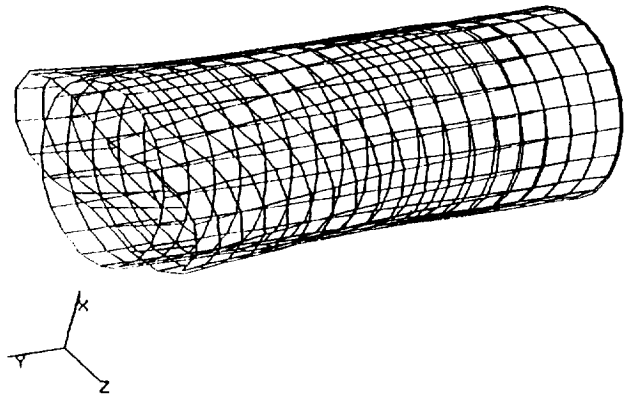

Figure 10. *The second mode shape of the* $[\pm\theta]_2$ *angle-ply laminated shell.*

2. Second frequency: the mode shape of the second frequency is shown in Figure 10. It is a combination of torsional and breathing (or radial) modes.
3. Third frequency: the mode shape of the third frequency is shown in Figure 11. It is a combination of torsional, breathing (or radial) and axial (or longitudinal) modes. These mode shapes are summarized in Table 4 for convenience.

Effects of the Laminate Thickness

The influence of the laminate thickness of the thin composite shell versus the ply angle θ for the three different laminate thickness ratios R/t of 20, 33.3 and 100 are presented in Figure 12. The computed values are normalized with respect to the maximum frequency of 264.4 cps. The following conclusions were reached from Figure 12.

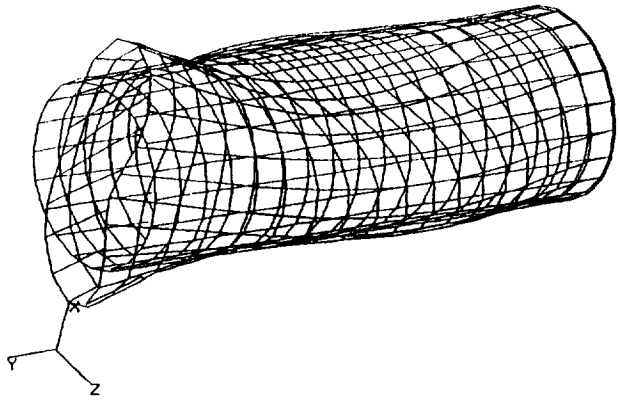

Figure 11. *The third mode shape of the* $[\pm\theta]_2$ *angle-ply laminated shell.*

Table 4. Mode shapes of the laminated shell (L/R = 6, R/t = 33.3 and fvr = 55%) as a function of the ply angle.

Laminate	First Frequency	Second Frequency	Third Frequency
$[0]_4$	Beam mode	Torsional and radial modes	Torsional, axial and radial modes
$[\pm 15]_2$	Beam mode	Torsional and radial modes	Torsional, axial and radial modes
$[\pm 22.5]_2$	Beam mode	Torsional and radial modes	Torsional, axial and radial modes
$[\pm 30]_2$	Beam mode	Torsional and radial modes	Torsional, axial and radial modes
$[\pm 45]_2$	Beam mode	Torsional and radial modes	Torsional, axial and radial modes
$[\pm 60]_2$	Beam mode	Torsional and radial modes	Torsional, axial and radial modes
$[\pm 75]_2$	Beam mode	Torsional and radial modes	Torsional, axial and radial modes
$[\pm 90]_2$	Beam mode	Torsional and radial modes	Torsional, axial and radial modes

1. For all R/t, the first natural frequencies increased for $0 \leq \theta \leq 15$ and decreased for $15 \leq \theta \leq 90$. The maximum frequency occurred at $\theta = 15$.
2. The thicker the composite shell the higher the values of the natural frequency. Thus thick composite shells ($R/t = 20$) had the highest frequencies, while thin composite shells ($R/t = 100$) had the lowest frequencies.
3. The percent difference of the natural frequencies between the thick laminated shell ($R/t = 20$) and the thin laminated shell ($R/t = 100$) are summarized in Table 5. As can be seen this difference is relative small.

Therefore, the influence of the laminate thickness ratio R/t had a small effect on the first natural frequency of the laminated shell.

Effects of Temperature

The effects of the temperature profiles through the laminate thickness on the free vibration in conjunction with the ply angle θ were examined. Three temperature profiles with uniform moisture (2 percent) were considered: the first profile was uniform with temperature equal to room temperature (21°C), the second profile was also uniform with temperature equal to $T_g/2$ (107.7°C) and the third profile was varying linearly, with temperature equal to $T_g/2$ in the inner surface and room temperature at the outer surface of the composite shell. The length ratio L/R was 4 and the laminate thickness ratio L/t was 33.3. The values of the first natural frequency are plotted versus ply angles θ and temperature profiles in Figure 13. The computed values of the first natural frequency were normalized with respect to the maximum value of 276.8 cps. The following observation are made.

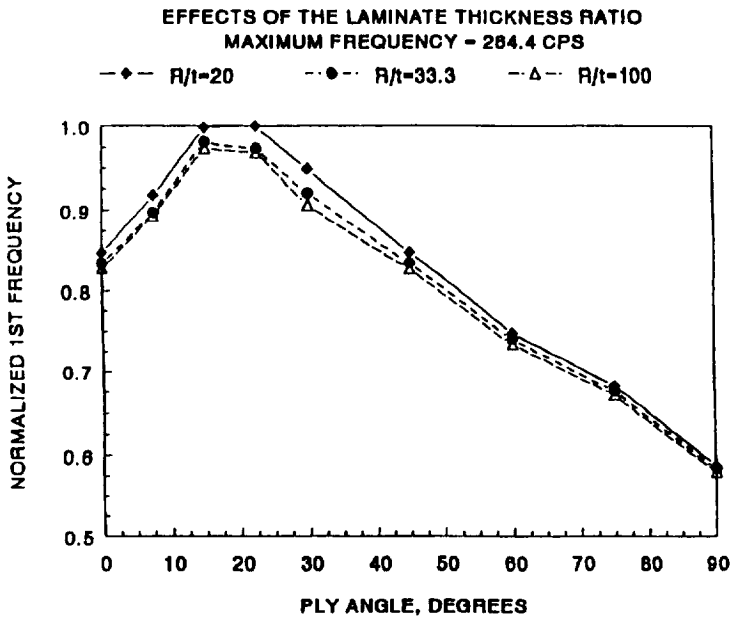

Figure 12. *Influence of the laminate thickness ratio* R/t *on the lowest frequency of the laminated shell.* L/R = 4, FVR = 55% *and moisture* = 2%.

1. For all temperature profiles, the natural frequencies increased for $0 \leq \theta \leq 20$ and decreased for $20 \leq \theta \leq 90$. The frequency peaked at $\theta = 20$.
2. The composite shell at room temperature had the highest frequencies, followed by the composite shell with the linear profile and finally the composite shell with the uniform temperature equal to $T_s/2$.
3. The percent difference in natural frequencies between the uniform profiles at room temperature and the $T_s/2$ temperature is low (Table 6), and is almost independent of the ply angle θ.

Therefore, the temperature profiles had a small effect on the natural frequency of the composite thin shell throughout the angle-ply range.

Table 5. The percent difference in the natural frequencies between the thick laminate (R/t = 20) and the thin laminate (R/t = 100).

Freq.	$[0]_4$	$[\pm 15]_2$	$[\pm 30]_2$	$[\pm 45]_2$	$[\pm 60]_2$	$[\pm 75]_2$	$[\pm 90]_2$
First	2.35%	2.5%	4.5%	9.62%	1.8%	0.8%	1.2%

$$\text{Percent difference} = \frac{\text{Frequency } (R/t = 20) - \text{Frequency } (R/t = 100)}{\text{Frequency } (R/t = 20)} \cdot 100\%$$

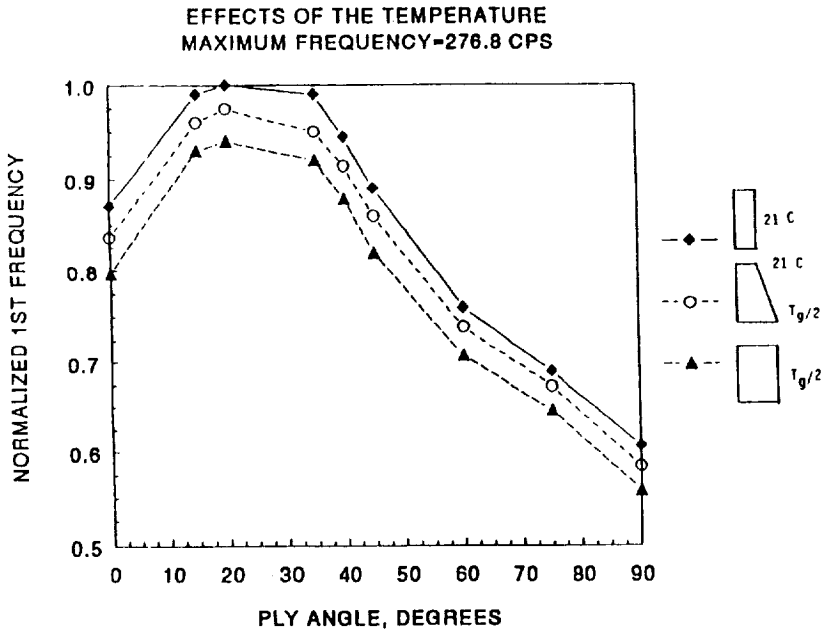

Figure 13. Influence of the temperature profile on the lowest frequency of the laminated shell. L/R = 4, R/t = 33.3, FVR = 55%, moisture = 2%.

Effects of Fiber Volume Fraction

The effects of the fiber volume fraction in conjunction with the ply angle θ on the free vibration behavior of the composite shell were evaluated. Three fiber volume fractions were examined: 55, 60 and 65 percent. The length ratio L/R was 4 and the laminate thickness ratio R/t was 33.3. The values of the first natural frequency are plotted for the different ply angles θ and for the various fiber volume fractions in Figure 14. The values of the natural frequency are normalized with respect the maximum value of 278.6 cps. The following conclusions were reached.

Table 6. The percent difference in the natural frequencies between the laminate shells in room temperature (T = 21 C) and in high temperature (T = T_G/2).

Freq.	$[0]_4$	$[\pm 15]_2$	$[\pm 30]_2$	$[\pm 45]_2$	$[\pm 60]_2$	$[\pm 75]_2$	$[\pm 90]_2$
First	3.8%	2.5%	3.1%	3.6%	3.3%	3%	3.5%

$$\text{Percent difference} = \frac{\text{Frequency } (T = 21\text{ C}) - \text{Frequency } (T = T_G/2)}{\text{Frequency } (T = 21\text{ C})} \cdot 100\%$$

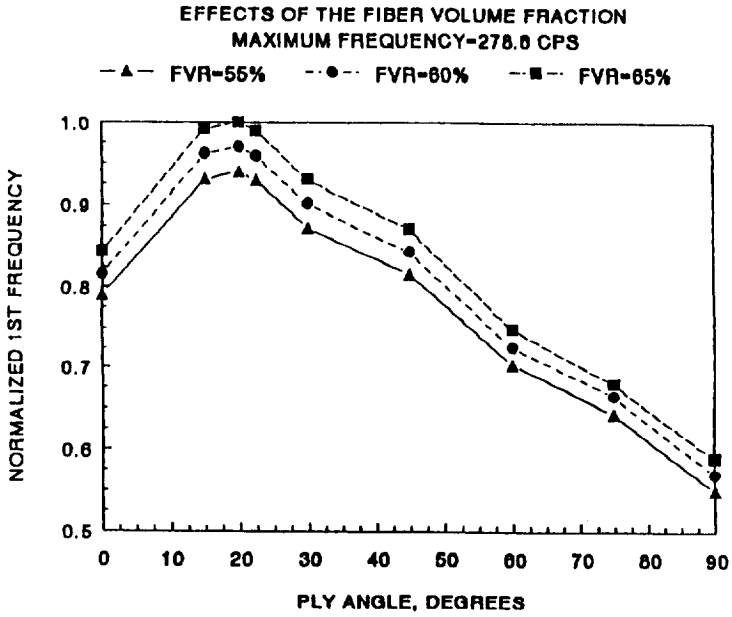

Figure 14. *Influence of the fiber volume fraction on the lowest frequency of the laminated shell.* L/R = *4,* R/t = *33.3, moisture = 2%.*

1. For all fiber volume fractions the natural frequencies increased for $0 \leq \theta \leq 20$ and decreased for $20 \leq \theta \leq 90$. The maximum natural frequency occurred at $\theta = 20$, which is the same for all the cases investigated.
2. The composite shell with the fiber volume fraction of 65 percent had higher frequencies than the shell with the fiber volume fraction of 60 percent which had higher frequencies than the shell with fiber volume fraction of 55.
3. The percent difference in the natural frequencies between the two laminates with fiber volume fraction of 65 and 55 is very low and is shown in Table 7.

Therefore, the influence of the fiber volume fraction had small effect on the natural frequency of the composite shell.

Table 7. The percent difference in the natural frequencies between the laminates with fvr of 65% and fvr of 55%.

Freq.	$[0]_4$	$[\pm 15]_2$	$[\pm 30]_2$	$[\pm 45]_2$	$[\pm 60]_2$	$[\pm 75]_2$	$[\pm 90]_2$
First	6.06%	6.05%	6.1%	6.3%	6.2%	5.4%	5.8%

$$\text{Percent difference} = \frac{\text{Frequency (fvr = 65\%)} - \text{Frequency (fvr = 65\%)}}{\text{Frequency } (R/t = 20)} \cdot 100\%$$

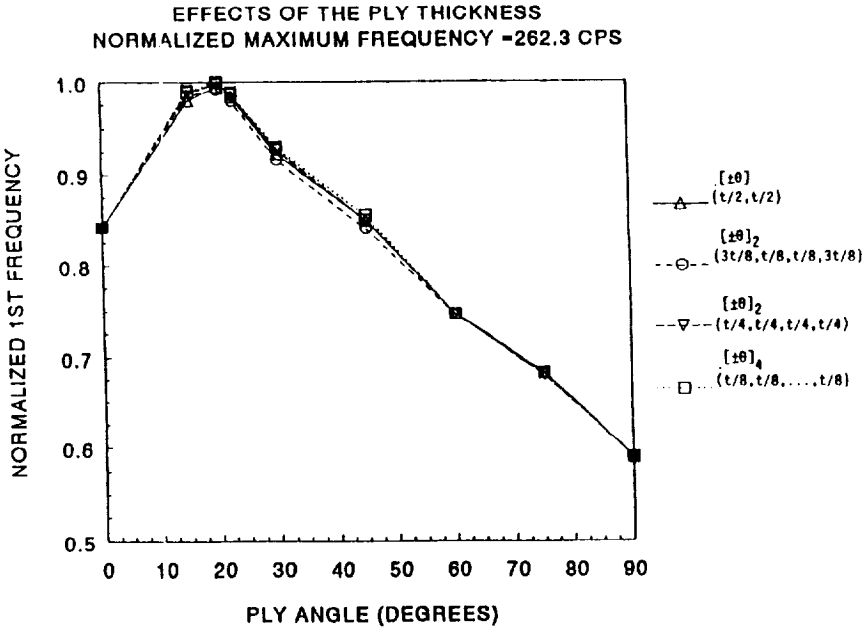

Figure 15. *Influence of the ply thickness on the lowest frequency of the laminated shell. L/R = 4, R/t = 33.3, FVR = 55%, and moisture = 2%.*

Effects of Ply Thickness

The effects of laminates with various ply thicknesses, in conjunction with the ply angle θ, were examined on natural frequencies of the composite shell. The length ratio L/R was 4, the laminate thickness ratio R/t was 33.3 and the fiber volume fraction was 55 percent. Four laminated shells with different ply thicknesses and the same laminate thickness (t) were examined: (1) a $[\pm\theta]$ angle-ply laminate with equal ply thicknesses ($t/2$, $t/2$); (2) a $[\pm\theta]_2$ angle-ply laminate with nonuniform ply thicknesses ($3t/8$, $t/8$, $t/8$, $3t/8$); (3) a $[\pm\theta]_2$ angle-ply laminate with uniform ply thicknesses ($t/4$, $t/4$, $t/4$, $t/4$); (4) a $[\pm\theta]_4$ angle-ply laminate with equal ply thicknesses ($t/8$, $t/8$, . . . , $t/8$). The computed values of the first natural frequency of these examined laminates are plotted for different ply angle θ in Figure 15. The following conclusions were reached.

1. The natural frequencies increased for $0 \leq \theta \leq 20$, decreased for $20 \leq \theta \leq 90$ and peaked at $\theta = 20$.
2. The laminate with different ply thicknesses had insignificant effect on the natural frequencies of the composite thin shell.

SUMMARY OF THE RESULTS

A computational simulation of the free vibration of hot, wet composite, thin

shells was performed by using a three-dimensional finite element analysis computer code.

The simulation included the effects of parameters such as ply angle, cylinder length, laminate thickness, temperature, fiber volume fraction and ply thickness on the free vibration behavior of the composite shells. The important results are summarized as follows.

1. The fiber orientations and the length of the laminated shell significantly influenced the free vibration behavior (frequencies and mode shapes) of the composite shell.
2. The fiber volume fraction, the laminate thickness and the temperature profile through the laminate thickness had a small effect on the free vibration behavior of the composite shell.
3. The laminates with different ply thicknesses had an insignificant effect on the free vibration behavior of the composite shell.
4. A single, through-the-thickness, eight-node, three-dimensional, composite finite element analysis appears to be sufficient for investigating the free vibration behavior of thin composite angle-ply cylindrical shells.

ACKNOWLEDGEMENT

The authors would like to thank Dr. Christos C. Chamis for his helpful discussion of the present paper.

REFERENCES

1. Hartle, M. 1990. *CSTEM User's Manual.* Cincinnati, OH: General Electric Company.
2. Gotsis, P. K. and J. D. Guptill. 1993. "Buckling Analysis of Laminated Thin Shells in a Hot Environment," NASA TM 106302.
3. Chamis, C. C. and S. N. Singhal. 1992. "Coupled Multi-Disciplinary Simulation of Composite Engine Structures in Propulsion Environments," NASA TM-105575.
4. Singhal, S. N., et al. 1993. "Coupled Multi-Disciplinary Composites Behavior Simulation," NASA TM-106011.
5. Singhal, S. N., et al. 1991. "Computational Simulation of Acoustic Fatigue for Hot Composite Structures," NASA TM-104379.
6. Murthy, P. L. N. and C. C. Chamis. 1986. "Integrated Composite Analyzer (ICAN)-User's and Programmer's Manual," NASA TP-2515.
7. Chamis, C. C. 1987. "Simplified Composite Micromechanics Equations for Hygral, Thermal and Mechanical Properties," NASA TM-83320.
8. Hurty, W. C. and M. F. Rubinstein. 1964. *Dynamics of Structures.* Prentice-Hall, Inc.
9. Meirovitch, L. 1967. *Analytical Methods in Vibrations.* The MacMillan Company.
10. Whitney, J. M., I. M. Daniel and R. B. Pipes. 1984. *Experimental Mechanics of Fiber Reinforced Composite Materials.* The Society for Experimental Mechanics.
11. Bathe, K. J. 1982. *Finite element Procedures in Engineering Analysis.* Prentice-Hall.
12. Zienkiewicz, O. C. 1977. The Finite Element Method, Third Edition. *McGraw-Hill Co.*